Off-Shell Model for Threshold Pionic η Production on a Nucleon and for ηN Scattering

R. S. Bhalerao and L. C. Liu
Isotope and Nuclear Chemistry Division, Los Alamos National Laboratory, Los Alamos, New Mexico 87545
(Received 29 October 1984)

An off-shell isobar model is presented for $\pi N \to \pi N$, $\pi N \to \eta N$, and $\eta N \to \eta N$ t matrices. The πN, ηN, and $\pi\Delta$ ($\pi\pi N$) channels are treated in a coupled-channels formalism. We are able to determine various vertex functions of the model by using only πN (complex) phase shifts in S_{11}, P_{11}, D_{13}, and P_{33} partial waves. The model gives good predictions for $\pi^- p \to \eta n$ cross sections. It also predicts an attractive S-wave ηN interaction.

PACS numbers: 13.75.−n

Pion-induced η production on a free nucleon is an important πN reaction in the energy region $T_\pi \simeq 0.6$–1.0 GeV. In terms of the cross-section magnitude, it is the second most important πN inelastic channel, second only to π-induced π production. Nuclear (π,η) reactions are also of great interest. In the SU(6) model, η differs from π^0 by having an additional $s\bar{s}$ quark-antiquark pair in its wave function. The systematics of ηN and $\pi^0 N$ scattering could yield information on the dynamical role of this $s\bar{s}$ pair in meson-baryon interactions. Like (γ,η) and other modes of nuclear η production, (π,η) reactions will enable one to study ηN scattering. Since hadronic and electromagnetic η-production processes are different, details of ηN scattering extracted from different types of nuclear reactions will complement each other. Because π^0 and η do not belong to the same isospin multiplet, comparative studies of $A(\pi,\eta)B$ and $A(\pi^\pm,\pi^0)B$ reactions are also of interest.

To date, little is known about nuclear (π,η) reactions, either theoretically or experimentally. In this Letter, we take the first step by presenting an off-shell model for the $\pi N \to \eta N$ t matrix, which can readily be used in nuclear (π,η) calculations. Our model will find immediate applications in the interpretation of $A(\pi^\pm,\eta)B$ data that will become available at the Clinton P. Anderson Meson Physics Facility (LAMPF) in the near future.[1]

The threshold for the reaction $\pi^- p \to \eta n$ on a free nucleon is at $T_\pi \simeq 561$ MeV or $\sqrt{s} \simeq 1488$ MeV. The total production cross section rises rapidly with pion energy and reaches a maximum (~ 2.5 mb) at $T_\pi \simeq 661$ MeV or $\sqrt{s} = 1550$ MeV.[2] For simple kinematic reasons, the threshold for nuclear (π,η) reactions is much lower. In the forthcoming LAMPF experiments pions of energies $T_\pi = 500$ to 550 MeV will be used. In this energy region, the basic $\pi N \to \eta N$ process is most likely to occur subthreshold. Existing theoretical models[3] for the $\pi N \to \eta N$ amplitude are based either on the K-matrix approach or on a Breit-Wigner-type parametrization with the masses and the partial widths of various resonances determined by fitting the experimental η-production cross sections. However, these models are not suitable for calculation of (π,η) reactions in a nucleus because they do not contain form factors to allow a meaningful off-shell extrapolation of the amplitude. They also cannot provide an ηN elastic-scattering amplitude, a quantity indispensible for calculating the final-state interaction in $A(\pi,\eta)B$ reactions. The model presented here overcomes these shortcomings. It is a coupled-channels, separable-interaction model in which reactions proceed via the formation of N^* or Δ isobars, and the interaction satisfies a relativistic Lippmann-Schwinger equation. Further, we do not fit but rather make predictions for $\pi^- p \to \eta n$ cross sections. The model also gives an ηN elastic-scattering amplitude.

In the energy region $\sqrt{s} = 1488$ to 1600 MeV, there are only three important channels in πN collision: $\pi N \to \pi N$, $\pi N \to \pi\pi N$, and $\pi N \to \eta N$. We incorporate all of them in our model. The diagrams for these interaction matrix elements are shown in Figs. 1(a) to 1(c), where α denotes N^* ($I = \frac{1}{2}$) or $\Delta(1232)$ (denoted henceforth as Δ) having a bare mass m_α. Because the ηN system has $I = \frac{1}{2}$, it can only couple to N^*. For the $\pi N \to \pi\pi N$ process, we follow Betz and Lee[4] and assume the dominance of the $\pi\Delta$ doorway state. In Figs. 1(a) to 1(c) each vertex is described by a vertex function $h^l_{a\alpha}(k)$ to be specified later. Here a denotes the channels πN, $\pi\Delta$, or ηN. The l and k denote respectively the relative orbital angular momentum and the magnitude of the c.m. momentum in channel a. Upon formal elimination of the $\pi\pi N$ channel, one obtains in the reduced model space a complex and energy-dependent effective interaction. The radial part of this interaction in a given partial wave l is

$$\langle p' | V^{\alpha l}_{ij}(\sqrt{s}) | p \rangle = \frac{h^l_{i\alpha}(p') h^l_{\alpha j}(p)}{\sqrt{s} - m_\alpha - \Sigma^\alpha_{2\pi}(\sqrt{s})}. \qquad (1)$$

Here $i = 1, 2$ and $j = 1, 2$, with 1 and 2 labeling respectively the πN and ηN channels. Because of parity and angular momentum conservation, V is diagonal in l. The appearance of $\Sigma^\alpha_{2\pi}(\sqrt{s})$ in Eq. (1) results from the formal elimination of the $\pi\pi N$ channel from our

model space. $\Sigma^{\alpha}_{2\pi}(\sqrt{s})$ is the self-energy of α, associated with a 2π intermediate state. It has two terms corresponding respectively to straight pion propagation [Fig. 1(d)] and crossed pion propagation [obtained from Fig. 1(d) by interchanging the right-hand ends of the pions]. This latter term contains an additional propagator and involves more complicated kinematics. To minimize algebraic complications in applying our model to nuclear reactions, we neglect the crossed term. However, because we determine h and m_α through fitting the πN phase shifts, effects of the crossed term will be phenomenologically included in the model parameters. We thus write our solution for $\Sigma_{2\pi}$ as

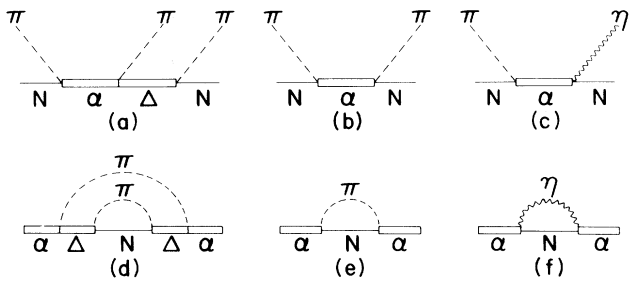

FIG. 1. (a)–(c) Schematic representation of the separable interaction matrix elements; (d)–(f) various contributions to the self-energy of a resonance α.

$$\Sigma^{\alpha}_{2\pi}(\sqrt{s}) = \int_0^\infty \sum_L \frac{[h^L_{\alpha,\pi\Delta}(q')]^2 q'^2\, dq'}{\sqrt{s} - E_{\pi q'} - E_{\Delta q'} - \Pi_\Delta(\sqrt{s},q') + i\epsilon},$$

with

$$\Pi_\Delta(\sqrt{s},q') = \int_0^\infty \frac{[h^1_{\Delta,\pi N}(q'')]^2 q''^2\, dq''}{\sqrt{s} - E_{\pi q'} - [(E_{\pi q''} + E_{Nq''})^2 + q'^2]^{1/2} + i\epsilon}.$$

Here, $E_{xq} \equiv (m_x^2 + q^2)^{1/2}$ is the energy of the particle x. The full solution of the coupled-channels equation $T = V + VG_0T$ with V of Eq. (1) is

$$\langle p'|T^{\alpha l}_{ij}(\sqrt{s})|p\rangle = \frac{h^l_{i\alpha}(p')\, h^l_{\alpha j}(p)}{\sqrt{s} - m_\alpha - \Sigma^{\alpha}_{\pi}(\sqrt{s}) - \Sigma^{\alpha}_{\eta}(\sqrt{s}) - \Sigma^{\alpha}_{2\pi}(\sqrt{s})}. \tag{2}$$

In Eq. (2) Σ^{α}_{π} and Σ^{α}_{η} are the self-energies associated, respectively, with πN and ηN intermediate states [Figs. 1(e) and 1(f)]. We have

$$\Sigma^{\alpha}_{\pi}(\sqrt{s}) = \int_0^\infty \frac{[h^l_{\alpha,\pi N}(q)]^2 q^2\, dq}{\sqrt{s} - E_{\pi q} - E_{Nq} + i\epsilon},$$

and a similar expression for $\Sigma^{\alpha}_{\eta}(\sqrt{s})$. Our coupled-channels formalism yields $\pi N \to \pi N$ $(i=j=1)$, $\eta N \to \eta N$ $(i=j=2)$, and $\pi N \to \eta N$ $(i=2, j=1)$ amplitudes in a single calculation.

We have parametrized the vertex functions as

$$h^l(q) = \frac{g}{2^{1/2} s^{1/4}} [v_l(q/\Lambda)]^{1/2} \frac{\Lambda^2}{\Lambda^2 + q^2},$$

where $v_l(\rho) \equiv [\rho^2 n_l^2(\rho) + \rho^2 j_l^2(\rho)]^{-1}$ is the "penetration factor."[5] The v_l ensures a correct threshold behavior while the other factors ensure a correct high-energy behavior. The parameters of our model are g, Λ, and the bare mass m_α. We included $\pi N\Delta$, $\pi\Delta\Delta$, πNN^*, $\pi\Delta N^*$, and ηNN^* vertices, with N^* being S_{11}, P_{11}, and D_{13} πN resonances. We did not include the ηNN vertex because (a) the energy region we are interested in ($\sqrt{s} = 1488$ to 1600 MeV) is far from the nucleon mass, and (b) according to a recent experiment $g_{\eta NN}$ is nearly zero.[6]

We first determined the $\pi N\Delta$ and $\pi\Delta\Delta$ vertex functions and the bare mass of Δ by fitting the πN P_{33} phase shifts.[7-9] The resulting $g_{\pi N\Delta}$, $\Lambda_{\pi N\Delta}$, and m_Δ were then treated as fixed input in the determination of the parameters in the N^* channels. In general, we found two solutions for each of these channels. However, one of them could be readily eliminated because it gave unphysical $N^* \to \pi N$ and $N^* \to \eta N$ branching ratios. Although the πN scattering data alone cannot determine the signs of the coupling constants, g, the η-production data helped us fix these signs. Satisfactory fits were obtained in all cases; as an example, we display in Fig. 2 our fits for the P_{33} and S_{11} channels. We summarize in Table I the parameters determined in this work.

We found that $g_{\pi N\Delta}/g_{\pi\Delta\Delta} = 1.9$ in good agreement with the ratio 2.1 predicted by the SU(4) model with point interactions.[11] We note also from Table I that πN phase shifts in Refs. 7 and 9 led to very similar P_{11} and D_{13} parameters but rather different S_{11} parameters. In spite of these differences, the dressed masses $m_\alpha + \Sigma^{\alpha}_{\pi} + \Sigma^{\alpha}_{\eta} + \Sigma^{\alpha}_{2\pi}$ were found to be quite similar. We believe that the existence of different S_{11} phase-shift solutions (Fig. 2) is related to the fact that the ηN channel, which is strongly coupled to the $S_{11}(1535)$ resonance, has not been taken into account very well in the πN phase-shift analyses.

The $\pi N \to \eta N$ c.m. differential cross section has the form $d\sigma/d\Omega = |f(\theta)|^2 + |g(\theta)|^2$, with the spin-

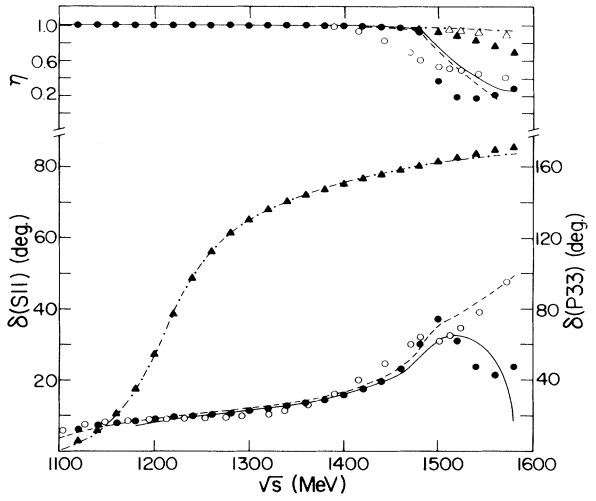

FIG. 2. πN scattering phase shifts δ (in degrees) and inelasticity parameters η vs $\sqrt{s}$. The S_{11} data of Ref. 9 (filled circles), the S_{11} data of Ref. 7 (open cirlces), and the P_{33} data of Ref. 9 (filled triangles), and of Ref. 7 (open triangles) are compared with the calculations shown respectively as the solid, dashed, and dot-dashed curves.

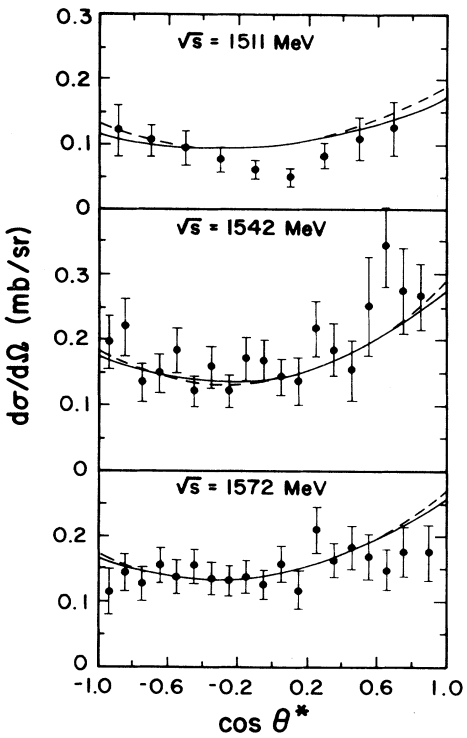

FIG. 3. Differential cross section for $\pi^- p \rightarrow \eta n$ vs cosine of the production angle in the c.m. frame. Solid (dashed) curves are obtained with parameters of Table I, based on πN phase shifts of Ref. 9 (Ref. 7). Data are from Ref. 2.

nonflip and spin-flip amplitudes f and g given by

$$f(\theta) = K[T_{S_{11}} + T_{P_{11}}\cos\theta + 2T_{D_{13}}P_2(\cos\theta)],$$

$$g(\theta) = K\sin\theta[T_{P_{11}} + 3T_{D_{13}}\cos\theta].$$

Here $K \equiv (\frac{2}{3})^{1/2}\pi(\mu_i\mu_f p_f/p_i)^{1/2}$ with p_i and p_f the initial and final c.m. momenta, θ the η-production angle, $\mu_i = E_{\pi p_i}E_{Np_i}/(E_{\pi p_i} + E_{Np_i})$, and $\mu_f = E_{\eta p_f}E_{Np_f}/(E_{\eta p_f} + E_{Np_f})$. The partial-wave production amplitudes $T_{S_{11}}$, $T_{P_{11}}$, and $T_{D_{13}}$ were calculated with Eq. (2).

TABLE I. Coupling constants g, range parameters Λ (in MeV/c), and bare masses m_α (in megaelectronvolts). Numbers with and without parentheses are due, respectively, to πN phase shifts of Refs. 9 and 7 (see Ref. 10).

Coupling to →		πN	$\pi\Delta$	ηN
P_{33}	g	(2.347)	(1.247)	· · ·
$m_\alpha = (1323.5)$	Λ	(331.0)	(264.9)	· · ·
S_{11}	g	1.384	3.509	0.616
$m_\alpha = 1608.1$		(1.301)	(7.080)	(0.769)
(2088.0)	Λ	344.3	203.3	465.1
		(435.2)	(376.6)	(1503.0)
P_{11}	g	1.814	5.019	0.267
$m_\alpha = 1588.6$		(1.988)	(4.989)	(0.305)
(1664.9)	Λ	568.9	110.4	207.1
		(573.5)	(159.8)	(187.9)
D_{13}	g	3.073	1.411	0.334
$m_\alpha = 1579.3$		(3.037)	(1.404)	(0.327)
(1567.8)	Λ	268.0	267.6	115.3
		(289.5)	(250.1)	(156.2)

The predicted $\pi N \rightarrow \eta N$ differential cross sections are compared with the experimental data[2] in Fig. 3. The agreement is excellent. As is clear from the expressions for f and g, the differential cross section based on $T_{S_{11}}$ and $T_{P_{11}}$ alone is angle-independent, while that based on $T_{D_{13}}$ alone has a minimum at $\theta = 90°$. Further, the differential cross section calculated with $T_{S_{11}}$ and $T_{P_{11}}$, but without $T_{D_{13}}$, can depend only linearly on $\cos\theta$, making it obvious that the structure in the experimental cross section reflects the presence of the D_{13} channel. This is in contrast to the conclusion drawn in Ref. 2 that below $\sqrt{s} = 1670$ MeV only S and P waves need be considered.

The S_{11}-wave ηN scattering lengths based on πN data of Refs. 7 and 9 are found to be $0.27 + i0.22$ and $0.28 + i0.19$ fm, respectively. The S_{11} ηN phase shifts have positive values, indicating an attractive S-wave interaction. The validity of this prediction will be checked with the forthcoming $A(\pi,\eta)B$ data.[1]

We conclude that our model is capable of describing the $\pi N \rightarrow \eta N$ reaction near threshold. We have noted that different πN phase-shift solutions can give very different g and Λ but very similar $\pi N \rightarrow \eta N$ cross sections. As different g and Λ imply different off-shell behavior of the interaction, we believe further studies of *nuclear* (π,η) reactions with our model will enable us to differentiate the qualities of various sets of πN phase shifts available in the literature.

This work was performed under the auspices of the Division of Nuclear Physics, U.S. Department of Energy. We thank Professor L. C. Biedenharn for bringing Ref. 6 to our attention, and Professor R. A. Arndt for making his πN phase shifts available to us prior to publication.

[1]J. C. Peng *et al.*, private communication.

[2]R. M. Brown *et al.*, Nucl. Phys. B **153**, 89 (1979).

[3]B. Carreras and A. Donnachie, Nucl. Phys. B **16**, 35 (1970), and references therein; P. N. Dobson, Phys. Rev. **146**, 1022 (1966); S. F. Tuan, Phys. Rev. **139**, 1393B (1965).

[4]M. Betz and T.-S. H. Lee, Phys. Rev. C **23**, 375 (1981).

[5]J. M. Blatt and V. F. Weisskopf, *Theoretical Nuclear Physics* (Wiley, New York, 1962).

[6]W. Grein and P. Kroll, Nucl. Phys. **A338**, 332 (1980).

[7]D. J. Herndon *et al.*, Lawrence Berkeley Laboratory Report No. UCRL-20030 πN (unpublished).

[8]G. Rowe, M. Salomon, and R. H. Landau, Phys. Rev. C **18**, 584 (1978).

[9]R. A. Arndt, private communication. We used this phase-shift solution FP84.

[10]The use of P_{33} phase shifts of Ref. 8 at T_π below 350 MeV, which give a better P_{33} resonance energy than Ref. 7, and the use of P_{33} phase shifts of Ref. 7 at higher energies led to parameter values very close to those given in Table I.

[11]G. E. Brown and W. Weise, Phys. Rep. **22**, 280 (1975).